

Theory of Hyperfine Fields at ^{57}Fe and ^{14}N Sites in Metmyoglobin and Related Compounds

S. K. Mun, Jane C. Chang,[†] and T. P. Das*

Contribution from the Department of Physics and Center for Biological Macromolecules, State University of New York at Albany, Albany, New York 12222.

Received December 8, 1978

Abstract: The electronic distributions in metmyoglobin, fluoromyoglobin, and a related compound, fluorohemepyrindine, are studied theoretically. The calculated electronic distributions are utilized to obtain the hyperfine fields at ^{57}Fe and ^{14}N nuclei. Data on the former are available in the first two compounds and in the five-liganded compound hemin, from Mössbauer and electron-nuclear double resonance (ENDOR) measurements and for the ^{14}N hyperfine constants in metmyoglobin and hemin from ENDOR measurements. Satisfactory agreement is found between the results of theory and experiment especially in terms of trends in going from one molecule to another and between different nitrogen nuclei in metmyoglobin. The electron distributions are also used to study the splitting of the iron 3s ESCA (electron spectroscopy for chemical analysis) in these compounds. From the charge and unpaired spin distributions over the molecules, it is concluded that the iron is strongly bonded to its ligands and that changes in the electron distributions in myoglobin and hemoglobin molecules due to changes in sixth ligands are channeled more strongly to the imidazole ligand of the histidine compound linked to the protein chain rather than to the porphyrin ring.

I. Introduction

The knowledge of the electronic structures of hemoglobin derivatives is important because it is expected to provide an understanding, at the microscopic level, of both the cooperative behavior¹ of the hemoglobin subunits during oxygenation and the effect of hydrogen ion concentration on oxygenation, known as the Bohr effect.² The hyperfine fields at ^{57}Fe and ^{14}N sites, which can be obtained experimentally from both Mössbauer experiments³ and electron-nuclear double resonance (ENDOR) experiments,⁴ give information on the distribution of unpaired electrons on these atoms in hemoglobin and related molecules. Theoretical work on the hyperfine fields at ^{57}Fe and ^{14}N nuclei in the hemoglobin-related systems is important both for the interpretation of the experimental data and for obtaining an in-depth understanding of the electronic distribution in these systems. In this paper we wish to present our theoretical work on the hyperfine fields at ^{57}Fe and ^{14}N nuclei in metmyoglobin (Met-Mb) (Figure 1), fluoromyoglobin (F-Mb), and a model compound, fluorohemepyrindine (F-Hm-Pyr).

From Mössbauer and ENDOR measurements, data are available on the hyperfine fields at ^{57}Fe in Met-Mb and F-Mb and hemin derivatives, and on the hyperfine fields at ^{14}N in Met-Mb and hemin derivatives. The experimental results are shown in Table I. It is seen that the hyperfine fields at ^{57}Fe in the three systems are very close to each other^{5,6} as also are the hyperfine fields at the $^{14}\text{N}_2$ nuclei of the porphyrin ring, while the ^{14}N hyperfine field assigned to the N_γ of the imidazole ring in Met-Mb is a factor of 1.5 times^{7,8} as large as the hyperfine field at the $^{14}\text{N}_2$ of the porphyrin ring. The work reported in this paper is aimed at elucidating the following features of the experimental data: (1) the near equality of ^{57}Fe hyperfine fields in Met-Mb, F-Mb, and hemin; (2) the near equality of the hyperfine fields at ^{14}N of porphyrin rings in Met-Mb and hemin; (3) the difference between the hyperfine fields at the ^{14}N nuclei in the porphyrin ring and in the imidazole in Met-Mb; (4) the smaller hyperfine constant of N_γ in F-Mb than Met-Mb; (5) the absolute magnitudes of the observed hyperfine fields in all these cases. In addition, we were interested in extracting useful general conclusions of chemical and biological significance from the consideration of both the experimental data and the results of our theoretical analysis.

In section II, we shall describe briefly the procedure we have

applied to obtain the electronic wave functions for these molecular systems and the hyperfine fields at ^{57}Fe and ^{14}N in them. In section III, we shall discuss our results and analyze how well they can explain the features of the experimental data. The concluding section (section IV) summarizes the general conclusions that one can arrive at from the present work.

II. Procedures

For the purpose of clarity, we shall divide this section into two parts. First, we shall describe the model systems that we have chosen as representative of the molecules of interest in the present work and the self-consistent charge-extended Hückel procedure⁹⁻¹¹ which we have used to obtain the molecular orbitals for these systems. In the second part, we shall consider the spin Hamiltonian¹² related to the hyperfine fields at the nuclei that is utilized to describe experimentally observed Mössbauer and magnetic resonance spectra. The procedure for relating the parameters of the spin Hamiltonian to the electronic wave functions of the molecules will be discussed in this second part of the present section.

A. The Self-Consistent Charge-Extended Hückel Method (SCCEH) for Determination of Electronic Wave Functions. The model systems that we have chosen for Met-Mb, F-Mb, and F-Hm-Pyr are respectively the compounds $\text{H}_2\text{O}-\text{Fe}(\text{III})$ -porphyrin-imidazole, $\text{F}-\text{Fe}(\text{III})$ -porphyrin-imidazole, and $\text{F}-\text{Fe}(\text{III})$ -porphyrin-pyridine, shown in Figure 1. For F-Mb the water molecule at the sixth ligand site is replaced by fluorine, and for F-Hm-Pyr the imidazole ligand is further replaced by a pyridine. The geometries of these molecules are chosen in keeping with the available X-ray data¹³⁻¹⁵ on Met-Mb and with some modifications to simplify the calculations. For all the three molecules we consider here, we have assumed reflection symmetry about the imidazole (or pyridine) plane with the latter bisecting the angle formed by the lines joining the center of the porphyrin ring to nitrogens on adjacent pyrrole rings on the porphyrin plane. For the F-Hm-Pyr system, there is twofold symmetry also about the plane perpendicular to the pyridine plane. The positions of the atoms on the porphyrin plane are chosen as before¹⁶ according to the crystal data of tetraphenylporphyrin.¹³ The bond lengths and bond angles of imidazole are taken from the X-ray data¹⁴ in Met-Hm or Met-Mb, while for the model compound F-Hm-Pyr the bond angles and the pyridine ligand are chosen from available information on free pyridine molecule.¹⁷ The locations of iron

[†] Singer Kearfott, Wayne, N.J. 07470.

Table I. Experimental Values of the Hyperfine Fields at ^{57}Fe and ^{14}N in Metmyoglobin (Met-Mb), Fluoromyoglobin (F-Mb), and Hemin

	A_{Fe}^{\perp} , MHz ^a	$A_{\text{N}_{\text{pp}}}^{\parallel}$, MHz	$A_{\text{N}_{\gamma}}^{\parallel}$, MHz
Met-Mb	27.41 ± 0.16	7.6 ± 0.02^b	11.46 ± 0.03^b
F-Mb	28.90 ± 0.16	^c	^c
hemin	26.42	6.84 ± 0.03	

^a A_{Fe}^{\perp} are the hyperfine constants for ^{57}Fe in MHz in the heme plane as obtained from Mössbauer spectra. The corresponding fields H_{Fe}^{\perp} are -498 ± 4 , -525 ± 3 , and -480 kOe for Met-Mb, F-Mb, and hemin, respectively. See ref 5. ^b $A_{\text{N}_{\text{pp}}}^{\parallel}$ and $A_{\text{N}_{\gamma}}^{\parallel}$ are the hyperfine coupling constants in megahertz at the ^{14}N nuclei of the porphyrin and imidazole nitrogens bonded to iron, respectively. See ref 7 and 8. ^c It was observed⁴⁴ that the general features of the nitrogen ENDOR from F-Mb are similar to those of Met-Mb. The main difference is that a readily identifiable higher frequency peak occurs about 0.5 MHz lower in frequency than that of Met-Mb which means that the $^{14}\text{N}_{\gamma}$ hyperfine coupling constant of F-Mb is about 1.0 MHz smaller than that of Met-Mb.

atoms for Met-Mb and F-Mb are chosen as being 0.229 \AA below the porphyrin plane toward the imidazole, as indicated by the X-ray data of metmyoglobin.¹⁴ The location of iron for F-Hm-Pyr is taken¹⁵ to be 0.3 \AA below the porphyrin plane, representing the average displacement of iron for high-spin six-liganded ferric heme systems obtained from X-ray data.

The electronic wave functions for the molecules are obtained through the SCCEH procedure.⁹⁻¹¹ The molecular orbitals ϕ_{μ} are expressed as linear combinations of the valence atomic orbitals χ_i of each atom in the molecule, according to

$$\phi_{\mu} = \sum_i C_{\mu i} \chi_i \quad (1)$$

where the molecular orbital coefficients $C_{\mu i}$ are obtained through the solution of the usual secular equation in the variational procedure, the secular equation involving Hamiltonian matrix elements $H_{ij} = \langle \chi_i | H | \chi_j \rangle$ and overlap matrix elements $S_{ij} = \langle \chi_i | \chi_j \rangle$.

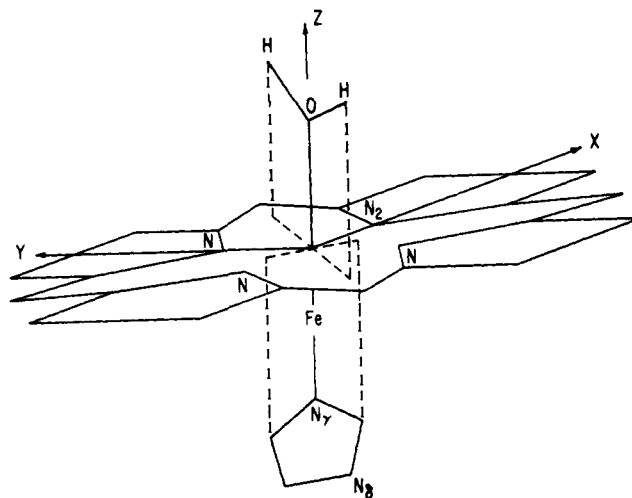
The Hamiltonian matrix elements H_{ij} are obtained semi-empirically⁷ in terms of the overlap integrals, ionization energies of the atoms in neutral and ionic states, and the charges on the atoms, the latter dependence introducing self-consistency in charge into the calculation. Thus, the charge q_l of the atom l is defined according to Mulliken's population convention as

$$q_l = - \sum_i^l [q_{li}^{\alpha} + q_{li}^{\beta}] + Z_l \quad (2)$$

where

$$q_{li}^{\alpha} = \sum_{\mu} \left[|C_{\mu i}|^2 + \sum_{m \neq l} \sum_j^m C_{\mu i} C_{\mu j} S_{ij} \right] n_{\mu}^{\alpha} \quad (3)$$

gives the electronic population for the i th atomic orbital with spin α on the l th atom, the dummy indices i, j denoting the atomic orbitals i, j of the l th and m th atom, respectively. Z_l represents the nuclear charge for the l th atom and n_{μ}^{α} the occupancy of the μ th orbital with spin α , with values 0 or 1 for empty or occupied orbitals, respectively. A similar expression holds for q_{li}^{β} in eq 2 for the atomic orbital with opposite spin β . The difference between q_{li}^{α} and q_{li}^{β} gives the unpaired spin population for the i th atomic orbital of the l th atom. In Table II, we have presented, for the three molecular systems studied, the electronic configurations of the following atoms: the iron atom, the nitrogen atom N_2 on porphyrin, the nitrogen atom N_{γ} that is directly bonded to iron and the other nitrogen atom, N_{δ} of imidazole and the sixth ligand atom bonded to iron (O in Met-Mb and F in F-Mb and F-Hm-Pyr; see Figure 1). For the sake of comparison we have also listed the iron and nitrogen

**Figure 1.** Molecular structure of H_2O -iron(III) porphyrin-imidazole, model system for metmyoglobin.

atom populations in the five-liganded high-spin heme system obtained in earlier work.¹⁶ The spin populations of the atomic orbitals which are related to the electron-nuclear magnetic hyperfine interactions, as discussed in the next section, can be obtained from Table II by taking the differences between the population for different spin states.

B. Theory for Evaluation of Hyperfine Fields at ^{57}Fe and ^{14}N Nuclei. The basic electron-nuclear magnetic hyperfine interaction Hamiltonian \mathcal{H}_{eN} is given by¹⁸

$$\mathcal{H}_{eN} = \mathcal{H}_{eN,\text{contact}} + \mathcal{H}_{eN,\text{dipolar}}$$

where

$$\mathcal{H}_{eN,\text{contact}} = \frac{8\pi}{3} \gamma_e \gamma_N \hbar^2 \mathbf{I}_N \cdot \sum_i \mathbf{s}_i \delta(\mathbf{r}_i)$$

and

$$\mathcal{H}_{eN,\text{dipolar}} = \gamma_e \gamma_N \hbar^2 \sum_i \frac{1}{r_i^5} [3(\mathbf{s}_i \cdot \mathbf{r}_i)(\mathbf{I}_N \cdot \mathbf{r}_i) - r_i^2 (\mathbf{I}_N \cdot \mathbf{s}_i)] \quad (4)$$

where \mathbf{I}_N and \mathbf{s}_i are the spin operators of the nucleus N and the electron i , respectively, \mathbf{r}_i is the position vector of the electron i with respect to nucleus N , and γ_e and γ_N are the gyromagnetic ratios of the electron and the nucleus N , respectively.

The first term in eq 4 is related to the contact hyperfine constant A_N while the second term gives rise to the dipole hyperfine term \mathbf{B}_N in the spin Hamiltonian:

$$\mathcal{H}^{\text{spin}} = \sum_N [A_N \mathbf{I}_N \cdot \mathbf{S} + \mathbf{I}_N \cdot \mathbf{B}_N \cdot \mathbf{S}] \quad (5)$$

Thus, from the basic electron-nuclear hyperfine interaction Hamiltonian \mathcal{H}_{eN} in eq 4, taking its expectation value over the determinantal many-electron wave functions and comparing with the matrix elements of $\mathcal{H}^{\text{spin}}$, one gets

$$A_n = (8\pi/3)(\gamma_e \gamma_N \hbar^2 / 2S) \sum_{\mu} [|\psi_{\mu\uparrow}(0)|^2 - |\psi_{\mu\downarrow}(0)|^2] \quad (6)$$

and corresponding expressions for the components of the second-rank tensor \mathbf{B}_N . For example, with the z direction taken as the direction perpendicular to the porphyrin plane, the component of \mathbf{B}_N is given by

$$B_{Nzz} = (\gamma_e \gamma_N \hbar^2 / 2S) \sum_{\mu} [\langle \psi_{\mu\uparrow}(\mathbf{r}) | (3 \cos^2 \theta - 1) / r^3 | \psi_{\mu\uparrow}(\mathbf{r}) \rangle - \langle \psi_{\mu\downarrow}(\mathbf{r}) | (3 \cos^2 \theta - 1) / r^3 | \psi_{\mu\downarrow}(\mathbf{r}) \rangle] \quad (7)$$

In eq 5-7 S is the total electronic spin of the molecule. The functions $\psi_{\mu\uparrow}(r)$ and $\psi_{\mu\downarrow}(r)$ represent respectively the molecular orbital wave function of the up and down spin molecular orbitals for the state μ , $|\psi_{\mu\uparrow}(0)|^2$ and $|\psi_{\mu\downarrow}(0)|^2$ being the electron densities at the nucleus N due to these molecular orbitals. On the right-hand side of eq 6, the difference in the bracket gives the net unpaired electron density at the nuclear site N due to orbital μ , the summation in μ being taken over all the valence molecular orbitals and the core state orbitals as well, the latter being represented very well by free atom

$$A_{Nc} = \frac{\sum_{\mu(\text{unpaired})} \sum_n \sum_k \left(\psi_{\mu}^{(1)} \psi_{ns}^{(2)} \left| \frac{1}{r_{12}} \right| \psi_{\mu}^{(2)} \psi_{ks}^{(1)} \right) \langle \psi_{ks} | \mathcal{H}_{eN, \text{contact}} | \psi_{ns} \rangle}{\epsilon_{ns} - \epsilon_{ks}} = \sum_n \sum_{\mu} \left(\psi_{\mu}^{(1)} \psi_{ns}^{(2)} \left| \frac{1}{r_{12}} \right| \psi_{\mu}^{(2)} \delta \psi_{ns}^{(1)} \right) \quad (10)$$

orbitals. In eq 7 for the dipolar term B_{Nzz} in the spin Hamiltonian, θ is the polar angle of the electron with respect to the nucleus N .

We consider the contact hyperfine constant A_N first. In principle, if both the valence and core electron orbitals were included in the expansion of the molecular orbital wave function in eq 1, and the Coulomb and exchange interactions are

$$A_{Nv} = \frac{\sum_{\mu(\text{unpaired})} \sum_{\nu} \sum_{\kappa} \left(\psi_{\mu}^{(1)} \psi_{\nu}^{(2)} \left| \frac{1}{r_{12}} \right| \psi_{\mu}^{(2)} \delta \psi_{\nu}^{(1)} \right) \langle \psi_{\kappa} | \mathcal{H}_{eN, \text{contact}} | \psi_{\nu} \rangle}{E_{\nu} - E_{\kappa}} = \sum_{\mu(\text{unpaired})} \sum_{\nu} \left(\psi_{\mu}^{(1)} \psi_{\nu}^{(2)} \left| \frac{1}{r_{12}} \right| \psi_{\mu}^{(2)} \psi_{\kappa}^{(1)} \right) \quad (11)$$

properly incorporated in the Hartree-Fock procedure utilized to obtain the molecular orbitals, then we would have the unrestricted Hartree-Fock (UHF) approximation²⁰ where the orbitals of different spins experience different exchange interactions. In such a case, the wave functions of valence and core electrons with different spins will be different and eq 6 could give the unpaired core and valence electron densities and hence the net hyperfine field. However, UHF calculations for large molecules would require a tremendous amount of time and effort. The molecular orbitals obtained from the SCCEH method⁹⁻¹¹ describe instead the orbitals of the valence electrons only, in the restricted Hartree-Fock (RHF) approximation, which assumes that the orbitals in the molecule are the same as the RHF orbitals in the atoms. If one confined oneself strictly to the RHF approximation, the contact hyperfine field at the ^{57}Fe nucleus could arise only from the spin density at ^{57}Fe from the unpaired molecular orbitals. This contribution to A_N will be designated as A_{Nd} in the following. The polarization of core electrons due to their exchange interaction with the unpaired valence electrons, which is included in the UHF procedure, would be absent from the spin density in eq 6 and has to be incorporated separately. For the hyperfine field at ^{57}Fe in high-spin ferric heme derivatives this is expected to be a large effect due to the influence of the exchange potential from the five unpaired valence electrons on the core electrons and, in fact, it is known both theoretically and experimentally to be the most important contribution to the ^{57}Fe hyperfine constant in free iron atom,²¹ ionic ferric compounds,²² and ferric heme derivatives.^{19,23,24} In addition to the exchange core polarization, there could also be an exchange polarization effect involving the influence of the five unpaired spin-valence electrons on the various paired valence orbitals.²⁵ This effect shall be termed the valence exchange polarization effect in the rest of the paper.

Thus, the net contribution to the hyperfine field at a nucleus, when one starts with the RHF approximation, can be written as the sum of the direct contribution A_{Nd} , exchange core polarization (ECP) contribution A_{Nc} , and exchange valence polarization (EVP) A_{Nv} , namely

$$A_N = A_{Nd} + A_{Nc} + A_{Nv} \quad (8)$$

The expression for A_{Nd} is similar to eq 6 except that one only uses the spin density at the nucleus from the unpaired spin orbitals, that is

$$A_{Nd} = \frac{8\pi}{3} \frac{\gamma_e \gamma_N \hbar^2}{2S} \sum_{\mu(\text{unpaired})} |\psi_{\mu}(0)|^2 \quad (9)$$

For A_{Nc} in atomic systems, both differential equation^{26,27} as well as conventional perturbation theory approaches²⁸⁻³⁰ have been used successfully in the literature. Thus one can write for A_{Nc} the two alternate forms

The summation over n in eq 10 of course refers to all the occupied core ns states and that over ks to excited ks states. In the second form of eq 10 $\delta \psi_{ns}$ refers to the first-order perturbation in the wave function for the ns core state due to the action of the perturbation Hamiltonian $\mathcal{H}_{eN, \text{contact}}$, which can be obtained by a differential equation procedure.^{26,27}

The expressions for A_{Nv} are very similar to eq 10, namely

the summation of ν referring to all the occupied paired spin valence states and over κ to the excited states. Since the ψ_{ν} are multicenter molecular orbitals, one cannot obtain $\delta \psi_{\nu}$ as in the atomic case by solving the differential equation of first-order perturbation theory,²⁶ and alternate methods are necessary.

Considering the ^{57}Fe nucleus first, the direct contribution A_{Nd} can be obtained from eq 9 using the calculated molecular orbital wave functions ψ_{μ} for the unpaired spin electrons. Since the iron 3d and 4p components of the molecular orbital wave functions have vanishing spin density at the ^{57}Fe nucleus, only the 4s component makes significant contribution, with a smaller additional contribution from the tail regions of the atomic orbitals of the ligand atoms. The evaluation of A_{Nc} and A_{Nv} by the first form of the right-hand side in eq 10 and 11 is impractical because it involves a knowledge of excited molecular state wave functions. One could use the second form for the case of A_{Nc} and A_{Nv} but this also leads in general to problems because of reasons discussed a little later for the ^{14}N hyperfine interaction, associated with the multicenter nature of the paired molecular orbitals. We have, therefore, utilized a pseudoatom approximation¹⁶ for both A_{Nc} and A_{Nv} for ^{57}Fe nucleus, which has been found to be quite satisfactory in earlier work on five-liganded heme compounds.

The pseudoatom approximation for A_{Nc} assumes this ECP contribution to be approximately proportional to the population of the unpaired valence orbitals on the atom under study, for example, the 3d orbitals in the case of iron atom. In this approximation, it is assumed that the radial characters of the core orbitals and the 3d orbital component of the valence electrons remain unchanged in the molecule as compared to the atom and consequently so does the exchange interaction between each core electron and a 3d valence electron on the iron atom. Hence the hyperfine field at the nucleus of the atom in question can be obtained from the known hyperfine field of the corresponding free atom by applying²³ the appropriate weighting factor, which is the ratio of the unpaired valence electron populations for the atom in the molecule and for the free atoms. In our analysis here, as in the earlier work on heme derivatives, we shall make use of the hyperfine interaction for iron atom in the $3d^7 4s^{1/2} 4s^{1/2} 4s^{1/2}$ configuration^{21,31} as the free atom reference system. A similar approximation is made for the exchange polarization contribution A_{Nv} to the ^{57}Fe hyperfine

Table II. Populations in Various Atomic Orbitals and Atomic Charges in Metmyoglobin (Met-Mg), Fluoromyoglobin (F-Mb), Fluorohemepyrindine (F-Hm-Pyr), and Hemin

		Met-Mb	F-Mb	F-Hm-Pyr	hemin
Fe	3d ↑	4.97	4.97	4.96	4.95
		1.83	1.97	2.01	1.79
	4s ↑	0.17	0.18	0.18	0.20
		0.17	0.18	0.17	0.20
	4p ↑	0.25	0.26	0.25	0.34
	0.21	0.21	0.19	0.27	
	atomic charge	0.40	0.23	0.25	0.25
N ₂	2s ↑	0.68	0.68	0.68	0.68
		0.67	0.67	0.67	0.67
	2p ↑	2.04	2.03	2.03	2.03
		1.84	1.81	1.80	1.80
	atomic charge	-0.23	-0.18	0.17	
N _γ	2s ↑	0.68	0.67	0.68	
		0.67	0.66	0.67	
	2p ↑	2.06	2.00	1.95	
		1.81	1.85	1.83	
	atomic charge	-0.22	-0.18	-0.13	
N _δ	2s ↑	0.68	0.62		
		0.67	0.62		
	2p ↑	2.05	1.91		
		1.88	1.90		
	atomic charge	-0.28	-0.05		
X ^a	ns ↑	0.77	0.97	0.97	1.82
		0.77	0.97	0.97	1.82
	np ↑	2.49	2.98	2.98	2.90
		2.33	2.67	2.66	2.51
	atomic charge	-0.38	-0.59	-0.59	-0.24

^a X is the sixth ligand of Fe in these systems (oxygen in Met-Mb, and fluorine in F-Mb and F-Hm-Pyr), and the fifth ligand chlorine in hemin. $n = 2$ for oxygen and fluorine, and $n = 3$ for chlorine.

field from the Fe 4s components of the paired valence electron molecular orbitals, which is the only component of these orbitals having finite density at the nucleus and hence the only component capable of making exchange polarization contribution to the hyperfine constant (through exchange interaction with the unpaired valence electrons). In this case, since the net population of the 4s orbitals on the Fe atom in the molecules is smaller than in the free atom, in contrast to the case of core states, an additional weighting factor corresponding to the ratio of this paired spin 4s population to that in the free atom has to be applied in obtaining the exchange polarization contribution to the ⁵⁷Fe hyperfine constant.

Thus the following expressions are used for A_{Nc} and A_{Nv} in the pseudoatom approximation:

$$A_{Nc} = q_{3d}^{\alpha} A_{3d,c} \quad (12)$$

$$A_{Nv} = 2q_{4s}q_{3d}^{\alpha} A_{3d,4s} \quad (13)$$

where q_{3d}^{α} refers to the net unpaired spin population in the iron atom 3d state, q_{4s} the spin population in either the α or β spin state from the paired spin valence molecular orbitals. The quantity $A_{3d,c}$ refers to the net exchange core polarization contribution to the hyperfine field in the reference configuration used for the iron atom and $A_{3d,4s}$ to the 4s contribution from the half-filled 4s shell in the reference.³¹ As will be seen in section III, the exchange core polarization term A_{Nc} makes the dominant contribution to the isotropic hyperfine constant for ⁵⁷Fe, with the exchange valence polarization term A_{Nv} the next in order of importance and the direct term A_{Nd} the smallest.

The components of the dipolar interaction tensor in eq 7 involve the anisotropy in the unpaired electron spin distribution around the particular nucleus in question. As in the case of the contact interaction constant, the components of B_N also are composed of direct and exchange polarization contributions. The exchange polarization contribution to the dipolar constants, because of the anisotropic nature of the electron-nuclear dipolar interaction Hamiltonian in eq 4, are more difficult to calculate than the isotropic hyperfine constant. Also in a few

cases^{29,32} where the anisotropic exchange polarization contributions have been calculated in atoms, they are significantly smaller than the direct contribution. For these reasons, the exchange polarization contribution to the dipolar hyperfine constant has not been included in our calculation. It should also be pointed out that for the isotropic hyperfine constant A_N , of ⁵⁷Fe, the direct contribution is very small, by virtue of the fact that the unpaired valence wave functions have primarily 3d character on the iron atom so that the exchange polarization contribution A_{Nc} is of paramount importance. On the other hand, for the ⁵⁷Fe dipolar hyperfine constant (which is found experimentally⁸ to be substantially smaller than the isotropic constant), the direct dipolar contribution is finite. For this reason, as well as the fact the exchange polarization contributions to the dipolar hyperfine interaction in atoms are known to be small,^{29,32} the importance of the exchange polarization contribution for the dipolar hyperfine interaction in the present systems is expected to be relatively less compared to the isotropic case.

For the ¹⁴N hyperfine constant, the direct contribution to the isotropic hyperfine constant can be obtained from eq 6 using the wave functions for the unpaired spin electrons. Since, unlike the case of iron atom where the atomic 4s orbital component of the molecular orbitals is small, the nitrogen 2s orbital character in the molecular orbitals is important, one therefore expects a sizable direct contribution from the unpaired spin orbitals. The exchange polarization effect is, however, difficult to include for nitrogen for the following reasons. In nitrogen atoms, the core 1s and 2s states produce sizable exchange polarization contributions of opposite sign leading to a net hyperfine constant which is a small fraction of the individual core contributions. In the molecule, we expect a similar cancellation between the ECP contribution associated with the 1s state and the EVP contributions from the paired orbitals, since the paired orbitals involve substantial 2s character. However, as we can see from eq 11, the evaluation of the EVP contribution requires a knowledge of $\delta\psi_{\nu}$, the perturbation of the paired valence states ψ_{ν} by the hyperfine Hamiltonian $\mathcal{H}_{eN,contact}$ (or alternatively a sum over the excited valence states ψ_{ν}). Since the ψ_{ν}

involve strong admixtures of 2p and 2s orbitals on the nitrogen atoms as well as neighboring atom orbitals, one cannot use the moment-perturbation procedure developed for core states,⁴⁷ involving states of definite angular momentum l in isolated atoms, to obtain $\delta\psi_v$. The pseudoatom approximation is also not satisfactory for the EVP contribution for ¹⁴N nucleus owing to the strong mixing between the 2p and 2s state orbitals of nitrogen atom. On the other hand, the 1s core ECP contribution can, of course, be obtained by the moment perturbation procedure,^{26,27} but, since one expects significant cancellation between the EVP contribution and 1s ECP contribution, and one cannot evaluate the former accurately without very substantial additional efforts involving summation over excited states k in eq 11, we have in the present work decided to omit both ECP and EVP contributions for ¹⁴N nuclei. This omission is not expected to be as serious here as it would be in the case of the ⁵⁷Fe nucleus, because in contrast to the latter, where the direct contribution is rather small so that exchange polarization effects are most important, in the present case we have very significant direct contribution. Our approach then, as in our earlier work¹⁹ on five-liganded heme derivatives, is to study the direct term for ¹⁴N hyperfine interaction to see how well it can explain the trends of variation in ¹⁴N hyperfine constants for porphyrin and histidine nitrogen atoms in metmyoglobin and also the trend it provides for the variation of these ¹⁴N hyperfine constants between met- and fluoromyoglobin systems. As discussed in section III, the comparison of the experimental ¹⁴N hyperfine constants and the combination of the direct contact dipolar terms can provide information regarding the net contribution from EVP and ECP terms in the molecule as in previous work on five-liganded systems.

Also, as in the case of ⁵⁷Fe hyperfine fields, for the ¹⁴N dipolar hyperfine tensor components, we have only evaluated the direct contributions to the dipolar hyperfine tensor \mathbf{B}_N for the nitrogen atoms. In evaluating this direct term one can get local effects arising from only the 2p atomic orbitals of the nitrogen atom in question and nonlocal and distant effects which also involve the orbitals on other atoms. The local contribution is known from earlier work on hemin derivatives¹⁹ to be the dominant one and it is sufficient to use it alone for \mathbf{B}_N .

III. Results and Discussion

Before discussing specifically our results for the hyperfine fields (interaction constants) at the ⁵⁷Fe and ¹⁴N nuclear sites, it is interesting to briefly analyze the electronic populations in the different orbitals of the nitrogen and iron atoms obtained from our calculation and the charges and unpaired spin populations on these atoms that are derived from the electronic wave functions.

These quantities are listed in Table II together with the corresponding quantities in hemin from earlier calculations. The charges on the various atoms in all these molecular systems investigated indicate that the atoms do not depart substantially from neutrality, in common with earlier conclusions on hemin.¹⁶ This is particularly significant for the iron atom, where the charge is close to 0.25 in all four systems instead of the value of 3.0 that would apply if the iron atom existed as a Fe³⁺ ion. This substantial departure of the charge on the iron atom from that expected for a Fe³⁺ ion shows that iron atom is bound quite strongly to its ligands. An important consequence of this strong bonding is the transfer of unpaired spin population from the iron atom to the ligands which has important influence on the hyperfine and other properties associated with these atoms, as will be discussed in this section.

The other noticeable feature of the charge distributions is that they do not vary significantly among the four molecules as far as atoms on the porphyrin plane are concerned, particularly the nitrogen atoms. The charges on the nitrogen atoms in the imidazole and pyridine ligands in Met-Mb, F-Mb, and

F-Hm-Pyr do, however, show somewhat more variations in going from one system to another.

Turning next to the unpaired spin populations on the atoms, it can be seen from Table II that, for the iron atom, the unpaired spin populations are respectively 3.16, 3.05, and 3.02 for Met-Mb, F-Mb, and F-Hm-Pyr, close to the corresponding population of 3.23 for hemin. On comparing these populations with the value of 5 expected if all the unpaired spins were localized on the iron atom, as in Fe³⁺ ion, one finds that there is substantial delocalization of the unpaired spin population away from the iron atom with some of the population that is drained from the iron atom appearing on the ligand atoms, especially the nitrogens. Thus, the picture of strong bonding between the iron atom and its ligands as demonstrated by the charge distributions on the atoms in the four molecules is also supported by the unpaired spin distributions on the atoms. There is experimental support for this delocalization of the unpaired spin away from the iron atom from ESCA measurements. Thus, in hemin, the iron 3s ESCA is observed experimentally³⁴ to be split into two lines with separation (2.4 ± 0.07) eV. This splitting originates³⁵ from the difference in exchange interaction energy of the two 3s electrons with different spin, the electron in the 3s state with spin parallel to the unpaired spin valence electrons being able to interact through exchange with these valence electrons while the electron in the 3s state with antiparallel spin cannot. The splitting is expected to be proportional to the unpaired spin population³⁶ on the iron atom and the fact that the experimental splitting is about half of the value of nearly 6 eV observed³⁷ for ionic compounds, with spin $\frac{1}{2}$ for the Fe³⁺ ion, already supports qualitatively the picture of transfer of spin population away from the iron due to its strong bonding with the ligand atoms. Actually there is also some quantitative support in this respect from the results of our earlier work on hemin.³⁸ From the calculated spin population on iron atom in hemin and using the average observed value 6.0 eV of the 3s ESCA splitting in ionic ferric compounds, the theoretical 3s splitting in hemin was found³⁸ to be 3.9 eV, in fair agreement with the experiments³⁴ in this system. Using the spin population on the iron atom in the other three compounds, we obtain for the 3s core ESCA splitting in Met-Mb, F-Mb, and F-Hm-Pyr the values 3.8, 3.7, and 3.6 eV, respectively. It would be helpful to have experimental ESCA data in these three molecules to test these theoretical values, at least the important feature of their closeness to the 3s ESCA splitting in hemin.

We turn next to the hyperfine interactions of the ⁵⁷Fe and ¹⁴N nuclei. Using the procedures described in section IIB the calculated contributions to the isotropic hyperfine field A at the ⁵⁷Fe nucleus, and the components of the dipolar hyperfine field tensor \mathbf{B} in the coordinate axes system in Figure 1, are listed in Table III, together with the corresponding results for hemin from earlier work.^{19,23,24} The experimental values of the hyperfine fields at the ⁵⁷Fe site in hemin, Met-Mb, and F-Mb from Mössbauer measurements^{5,6} are also listed in the last column for comparison with theory. Mössbauer measurements^{5,6} provide the hyperfine field on the plane of the porphyrin ring and so the theoretical values $A + B_{xx}$ are tabulated in the sixth column for comparison with experiment.³⁸ The theoretical results are seen to be in reasonable agreement with experiment, with both the theoretical and experimental values in all three systems being close to each other as expected from the closeness of the unpaired spin populations in the iron 3d orbitals in these systems. The somewhat poorer agreement between experiment and theory for F-Mb as compared to that for Met-Mb and hemin may be due to either a possible underestimation in A or overestimation in B_{xx} . The latter possibility is a little more likely than the former, because A involves the isotropic component of the spin density about the ⁵⁷Fe nucleus, while the dipolar tensor involves the anisotropic

Table III. Theoretical Results for the Components of Hyperfine Field at ^{57}Fe in Metmyoglobin (Met-Mb), Fluoromyoglobin (F-Mb), Fluorohemepyrindine (F-Hm-Pyr), and Hemin (kOe)

molecules	A_d	A_c	A_p	A	$B_{zz},$ $B_{yy},$ B_{xx}	$(A + B_{xx})^a$	$(H_{\text{exp}})^b$
Met-Mb	1.9	-546.7	35.3	-509.5	-51.2 25.6 25.6	-483.9	-498 ± 4
F-Mb	1.7	-523.5	35.8	-486.0	-67.7 33.8 33.8	-452.2	-525 ± 3
F-Hm-Pyr	1.8	-512.9	34.4	-479.7	-72.6 40.3 32.3	-447.4	
hemin				-507.1	-49.0 24.5 24.5	-482.6	-480

^a For comparison with the Mössbauer hyperfine field in polycrystalline material one should take an average of $A + B_{xx}$ and $A + B_{yy}$. However, since B_{xx} and B_{yy} do not differ substantially, we have listed only $A + B_{xx}$ for comparison with experiment. ^b The experimental values for Met-Mb, F-Mb, and hemin are from ref 5 and 6.

Table IV. Theoretical Results for the ^{14}N Hyperfine Constants (MHz) at the N_2 , N_ϵ , and N_δ Sites in Metmyoglobin (Met-Mb), Fluoromyoglobin (F-Mb), Fluorohemepyrindine (F-Hm-Pyr), and Hemin

molecule	N	A	B_{zz}	B_{xx}	B_{yy}	$(A + B_{zz})^a$	exptl
Met-Mb	N_2	5.47	-1.79	3.95	-2.16	3.68	7.60 ^b
	N_γ	4.53	3.65	-1.83	-1.83	8.18	11.46 ^b
	N_δ	2.66	0.44	-0.22	-0.22	3.10	
F-Mb	N_2	5.55	-1.96	4.34	-2.38	3.59	^c
	N_γ	3.63	2.96	-1.48	-1.48	6.59	^c
	N_δ	0.30	-0.03	-0.11	0.14	0.27	
F-Hm-Pyr	N_2	5.45	-2.04	4.52	-2.49	3.41	
	N_γ	2.89	2.91	-1.45	-1.46	5.78	
hemin	N_2	5.06	-1.26	3.83	-2.57	3.80	6.84

^a The ENDOR hyperfine fields refer to a direction perpendicular to the heme plane and, therefore, the $(A + B_{zz})$ are the approximate theoretical results to compare with experiment. ^b See ref 7 and 8. ^c See Table I and ref 42.

component which is connected with differences in unpaired spin populations in different d states of iron and is more susceptible in inaccuracy. It would be helpful in the future to study the anisotropic unpaired spin population distribution by other methods and by changes in the semiempirical Hamiltonian used in the extended Hückel approximation⁹⁻¹¹

Turning next to the ^{14}N hyperfine interaction, the contributions to the ^{14}N isotropic hyperfine constants and the components of the tensor \mathbf{B}_N , calculated following the procedure described in section IIB, are listed in Table IV for the porphyrin ^{14}N nuclei as well as the ^{14}N nuclei for the imidazole and pyridine ligands. The corresponding theoretical results^{16,19,24} for the porphyrin $^{14}\text{N}_2$ in hemin are also included for reference as also are the experimentally measured hyperfine fields for both $^{14}\text{N}_2$ and $^{14}\text{N}_\gamma$ for Met-Mb and F-Mb. The experimental results for the ^{14}N nuclei are obtained from the ENDOR measurements,⁸ so that the pertinent theoretical result to compare with in this case is $A + B_{zz}$. Considering first the results for ^{14}N nuclei in the porphyrin ring, the similar electronic distributions indicated by both the calculated charges and unpaired spin populations (Table II) are reflected in the similar values found for A and the components of B in all four systems (Table IV). This also leads to near equality of the hyperfine fields $A + B_{zz}$ in all four cases, in agreement with the experimental trend from porphyrin ^{14}N ENDOR data⁸ in Met-Mb and hemin. The other interesting result is the fact that the ^{14}N hyperfine constant associated with N_γ , the imidazole nitrogen atom liganded to iron in the three systems Met-Mb, F-Mb, and F-Hm-Pyr, is found to be substantially larger than that for the porphyrin nitrogen N_2 in all three molecules. A major reason for this is the reversal in sign of B_{zz} for N_2 and N_γ as a consequence of the geometry of the molecular systems. The pre-

dicted ratios of the ^{14}N hyperfine fields at N_γ and N_2 are found theoretically to be 2.2, 1.8, and 1.7 for Met-Mb, F-Mb, and F-Hm-Pyr, all substantially larger than unity, in essential agreement with the observed experimental ratio of 1.5 for Met-Mb and F-Mb. It is also interesting that the direction of change in the spin density on N_γ (Table II) due to change in the sixth ligand from H_2O to fluorine is also reflected in the observed change in the hyperfine constant of ^{14}N in the same direction. The near constancy of the ^{14}N hyperfine constant in the porphyrin ring in going from the fluoro to the met system is also verified experimentally, a feature that is similar to the insensitiveness of the spin density at porphyrin nitrogen to changes in fifth ligand in five-liganded systems. It would be helpful to have experimental results to check our prediction in Met-Mb and F-Mb for the hyperfine constants N_δ , the other nitrogen atom of the imidazole, besides N_γ which is bonded to the iron atom.

It should be remarked that, while the available experimental trends in the ^{14}N hyperfine data are well explained by the theoretical results in Table IV, the absolute values of the theoretical results are between 50 and 70% of the experimental values.^{8,9} This underestimation in the hyperfine fields at ^{14}N nuclei seems to be a common feature in a number of heme systems.^{39,40} One likely source for explaining the differences in theoretical and experimental absolute values is the influence of exchange core and valence polarization contributions for the ^{14}N nuclear hyperfine constants in these systems, which have not been included. The reason for not including these exchange contributions has been explained in section IIB. Thus in eq 11 for the exchange valence polarization, we now have the unpaired and paired spin electron state wave functions, ψ_μ and ψ_ν involving hybrid mixture of 2s and 2p states on the ni-

trogen atom instead of pure 2s states, as in the case of free nitrogen atom. Consequently, the evaluation of A_{EVP} requires either the moment-perturbed solution $\delta\psi$, for these paired states, which requires development of other procedures besides that used^{26,27} in the atom or a summation over excited states in the alternate expression for A_{ECP} in eq 11, which are not available. Since the EVP and ECP effects, the latter from the nitrogen atom 1s core electrons, were expected, as in the free atom,²⁸ to cancel each other substantially, it was not considered appropriate to include the ECP effect alone, though it could have been evaluated by the moment-perturbation procedure as used in solid-state calculations.^{26,27} However, a consideration of the expected nature of the ECP and EVP contributions indicates that their net effect would be positive, in the direction of reducing the difference between the direct contribution and experiment. Thus, in free nitrogen atom,²⁸ the unpaired electrons are in purely 2p states, and the outer paired electrons are in purely 2s states, so that the core polarization effect associated with the latter orbitals involves only 2p-2s exchange. However, since in the molecules the paired and unpaired molecular states involve hybridization of nitrogen 2p and 2s orbitals, one can now have the stronger 2p-2p and 2s-2s exchange operative, in addition to the 2p-2s exchange. The exchange polarization contribution from the paired 2s states in the atom is known²⁸ to be positive and overcomes the corresponding negative effect from the core 1s states, the sum representing a sizable part of the experimentally observed hyperfine constant in the atom.⁴¹⁻⁴³ Therefore, if one made the reasonable assumption that the exchange polarization contribution from the valence electrons in the molecules is also positive and larger in magnitude than that from the 2s states in the free atom, it appears that the hybridization of the 2p and 2s orbitals in the paired and unpaired orbitals in the molecule would provide the effect in the right direction to improve agreement with the experimentally observed results in Met-Mb. This effect needs, however, to be quantitatively investigated and will require the development of procedures to conveniently handle the exchange polarization effect for delocalized paired valence orbitals with comparable accuracy as for localized paired core orbitals.^{26,27}

IV. Conclusion

In summary then, from a theoretical analysis of the electronic structures and the hyperfine interactions of ⁵⁷Fe and ¹⁴N nuclei, it has been possible to explain the main features of the available experimental data. The first is the magnitudes of the ⁵⁷Fe hyperfine fields in Met-Mb, F-Mb, and hemin and the experimental trend that these magnitudes are close to each other.^{5,6} Secondly, one is able to explain the fact that the ¹⁴N hyperfine constant for the N_γ atom of the imidazole ligand in Met-Mb is found experimentally⁸ to be substantially larger than for the porphyrin nitrogen atom N₂. Thirdly, the experimental fact that the ¹⁴N hyperfine constants of N₂ in hemin and Met-Mb are close to each other^{7,8} is satisfactorily explained. Also, the observed decrease⁴⁴ in the ¹⁴N hyperfine constant in going from metmyoglobin to fluoromyoglobin is explained by our calculated results for the spin distribution.

From these observed satisfactory agreements between theoretical and experimental trends, we feel that the theoretical treatment adopted in the present work for obtaining the electronic wave functions has succeeded in providing a reasonably good overall description of the electron distributions over the molecules studied. Our result that the iron atom appears to be strongly bonded to the porphyrin and imidazole ligands, as evidenced by its near neutrality and substantial reduction of the unpaired spin population from that in a Fe³⁺ ion, indicates that the iron atom can communicate^{45,46} electronic changes produced by substitutions at the sixth ligand site (where oxygen is attached in hemoglobin) very effectively to its other ligands.

Also, the result that the electronic population on the nitrogen atom N_γ of the imidazole liganded to the iron changes significantly in changing ligands, as in going from Met-Mb to F-Mb, while that at N₂ on the porphyrin does not change appreciably, indicates that the changes in the electronic distribution in the hemoglobin molecule due to changes in the sixth ligands are channeled more to the imidazole component of the histidine linking the heme to the protein chain than to the porphyrin ring.

There are some remaining quantitative differences between experimental and theoretical hyperfine constants, the most significant being the ¹⁴N hyperfine constants in Met-Mb and F-Mb (Table I). In attempting to bridge this difference, as discussed in section III, we need the extension of the perturbation procedure, currently used for the study of exchange polarization effects associated with atomic core electrons,^{26,31,47} to apply to multicenter paired spin molecular orbital states.

Acknowledgment. The authors are very grateful to Professor Charles P. Scholes for valuable discussions and suggestions. This work was supported by a grant from the National Heart and Lung Institute.

References and Notes

- (1) E. Antonini and M. Brunori in "Hemoglobin and Myoglobin in Their Reactions with Ligands", American Elsevier, New York, 1971, Chapter 14.
- (2) E. Antonini and M. Brunori in ref 1, p 179.
- (3) See, for example, U. Gonser, "Mössbauer Spectroscopy", Springer-Verlag, New York, 1975.
- (4) G. Feher, *Phys. Rev.*, **103**, 500 (1956).
- (5) G. Lang, *Q. Rev. Biophys.*, **3**, 1 (1970); C. E. Johnson, *Phys. Lett.*, **21**, 491 (1966).
- (6) G. Lang, I. Asakura, and T. Yonetani, *Biochim. Biophys. Acta*, **214**, 381 (1970).
- (7) For fluoro-, chloro-, and bromohemin, see H. L. Van Camp, C. P. Scholes, and C. F. Mulks, *J. Am. Chem. Soc.*, **98**, 4094 (1976).
- (8) For metmyoglobin, see C. P. Scholes, R. A. Isaacson, and G. Feher, *Biochim. Biophys. Acta*, **263**, 448 (1972).
- (9) R. Hoffman, *J. Chem. Phys.*, **39**, 1397 (1963).
- (10) M. Zerner, M. Gouterman, and H. Kobayashi, *Theor. Chim. Acta*, **6**, 363 (1966).
- (11) J. C. Chang, Y. M. Kim, and T. P. Das, *Theor. Chim. Acta*, **41**, 37 (1976).
- (12) A. Carrington and A. D. McLachlan, "Introduction to Magnetic Resonance", Harper and Row, New York, 1967.
- (13) J. L. Hoard, M. J. Hamor, and T. A. Hamor, *J. Am. Chem. Soc.*, **85**, 2334 (1963).
- (14) H. C. Watson, *Prog. Stereochem.*, **4**, 299 (1969).
- (15) J. L. Hoard, *Science*, **174**, 1295 (1971).
- (16) P. S. Han, T. P. Das, and M. F. Rettig, *Theor. Chim. Acta*, **16**, 1 (1970).
- (17) L. E. Sutton, "Tables of Interatomic Distances and Configuration in Molecules and Ions", *Chem. Soc., Spec. Publ.*, No. 18 (1965).
- (18) T. P. Das, "Relativistic Quantum Mechanics of Electrons", Harper and Row, New York, 1973, Chapter 7.
- (19) M. K. Mallick, J. C. Chang, and T. P. Das, *J. Chem. Phys.*, **68**, 1462 (1978).
- (20) R. E. Watson and A. J. Freeman in "Hyperfine Interactions", A. J. Freeman and R. B. Frankel, Eds., Academic Press, New York, 1967, Chapter 2.
- (21) K. J. Duff and T. P. Das, *Phys. Rev. B*, **3**, 192, 2294 (1971).
- (22) S. N. Ray, T. Lee, and T. P. Das, *Phys. Rev. B*, **8**, 5291 (1973).
- (23) M. F. Rettig, P. S. Han, and T. P. Das, *Theor. Chim. Acta*, **12**, 178 (1968). Erratum: *ibid.*, **13**, 432 (1969).
- (24) M. K. Mallick, S. Mishra, J. C. Chang, and T. P. Das, Proceedings of Nassau Mössbauer Conference, C. I. Wynter and R. H. Herber, Eds., 1977, p 144.
- (25) J. E. Rodgers and T. P. Das, *Phys. Rev. A*, **8**, 2195 (1973).
- (26) G. D. Gaspari, W. M. Shyu, and T. P. Das, *Phys. Rev. A*, **134**, 852 (1964).
- (27) D. Ikenberry and T. P. Das, *Phys. Rev. B*, **2**, 1219 (1970).
- (28) N. C. Datta, C. Matsubara, R. T. Pu, and T. P. Das, *Phys. Rev.*, **177**, 33 (1969).
- (29) J. D. Lyons, R. T. Pu, and T. P. Das, *Phys. Rev.*, **178**, 103 (1969). Erratum: *ibid.*, **186**, 266 (1969).
- (30) J. E. Rodgers, Ph.D. Thesis, University of California, Riverside, 1972.
- (31) K. J. Duff and T. P. Das, *Phys. Rev. B*, **12**, 3870 (1975).
- (32) S. D. Mahanti and T. P. Das, unpublished.
- (33) C. P. Scholes, R. A. Isaacson, T. Yonetani, and G. Feher, *Biochim. Biophys. Acta*, **322**, 457 (1973).
- (34) G. K. Wertheim (unpublished) quoted by J. C. Chang, Y. M. Kim, and T. P. Das, *J. Chem. Phys.*, **62**, 4350 (1975).
- (35) A. J. Freeman, P. S. Bagus, and J. V. Mallow, *Int. J. Magn.*, **4**, 35 (1975).
- (36) The absolute value of the splitting is influenced also by difference in correlation effects [P. S. Bagus, A. J. Freeman, and F. Sasaki, *Phys. Rev. Lett.*,

- 30, 850 (1973)] in the two ionized states involving the ionization of 3s electrons with either spin but the assumption of proportionality to the unpaired valence population on the iron atom is still valid.
- (37) S. Hüfner and G. K. Wertheim, *Phys. Rev. B*, **7**, 2333 (1975).
- (38) The hyperfine field at Met-Mb is also available from ENDOR measurements (ref 29), the ENDOR results being in satisfactory agreement with the result from the Mössbauer measurements.
- (39) See ref 16, 23, and 24.
- (40) M. A. Heald and R. Berlinger, *Phys. Rev.*, **96**, 645 (1954).
- (41) W. W. Holloway and R. Novick, *Phys. Rev. Lett.*, **1**, 367 (1958).
- (42) L. W. Anderson, F. M. Pipkin, and J. C. Baird, *Phys. Rev.*, **116**, 87 (1959).
- (43) C. F. Mulks, C. P. Scholes, L. C. Dickinson, and A. Lapidot, *J. Am. Chem. Soc.*, **101**, 1645 (1979).
- (44) M. F. Perutz, *Nature (London)*, **228**, 726 (1970).
- (45) J. J. Hopfield, R. G. Shulman, and S. Ogawa, *J. Mol. Biol.*, **61**, 425 (1971).
- (46) C. M. Singal, B. Krawchuk, and T. P. Das, *Phys. Rev. B*, **16**, 5108 (1977).
- (47) This same limitation in principle applies to the case of EVP contribution from the paired states to the ^{57}Fe hyperfine constant, where the pseudoatom approximation used amounts to only considering the perturbation of the 4s components of paired valence electron molecular orbitals on the iron atom, which is not a serious approximation because the EVP contribution for the ^{57}Fe case is quite small and also no comparable cancellation occurs between EVP and ECP effects as in the case of ^{14}N .

Laser Photoelectron Spectrometry of the Negative Ions of Iron and Iron Carbonyls. Electron Affinity Determination for the Series $\text{Fe}(\text{CO})_n$, $n = 0, 1, 2, 3, 4$

P. C. Engelking[†] and W. C. Lineberger*

Contribution from the Department of Chemistry, University of Colorado, Joint Institute for Laboratory Astrophysics, University of Colorado, and National Bureau of Standards, Boulder, Colorado 80309. Received January 2, 1979

Abstract: With a fixed-frequency Ar ion laser, the photoelectron spectra of the negative ions Fe^- , FeCO^- , $\text{Fe}(\text{CO})_2^-$, $\text{Fe}(\text{CO})_3^-$, and $\text{Fe}(\text{CO})_4^-$ have been obtained. The electron affinity of iron is found to be (0.164 ± 0.035) eV while the electron affinities for other members of this series increase roughly as the number of ligands. Thus for FeCO the EA is (1.26 ± 0.02) eV; for $\text{Fe}(\text{CO})_2$, (1.22 ± 0.02) eV; for $\text{Fe}(\text{CO})_3$, (1.8 ± 0.2) eV; for $\text{Fe}(\text{CO})_4$, (2.4 ± 0.3) eV. In addition, the photoelectron spectra provide information on vibration frequencies, electronic states, and Fe-CO bond strengths in these compounds.

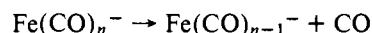
I. Introduction

Until recently¹ there had been no experimental determination of the atomic electron affinity (EA) of iron, although efforts have been made to estimate this quantity for iron and also for a number of other atoms for which it remains unmeasured.² We describe here a method for determining electron affinities directly and accurately by photoelectron spectrometry on beams of atomic or molecular anions. We apply this technique to determine the electron affinities of the carbonyl series $\text{Fe}(\text{CO})_n^-$ with $n = 0, 1, 2, 3$, or 4. These data afford a systematic study of successive ligand binding to a central metal atom.

Photodetachment of the negative ions of the iron carbonyls has been observed previously in ICR experiments of Richardson et al.³ and Dunbar and Hutchinson.⁴ Basically, the ions were trapped in an ion cyclotron resonance cell and their disappearance was monitored as a function of the intensity and wavelength of the irradiating light. There is some uncertainty about the nature of the photodisappearance, i.e., whether it is photodissociation by elimination of a CO group, or photodetachment by elimination of an electron. This question was partially answered by Richardson et al.³ by measuring the formation of the respective $\text{Fe}(\text{CO})_{n-1}^-$ ion upon irradiation of the $\text{Fe}(\text{CO})_n^-$ ion, indicating that photodissociation was occurring. However, it was uncertain whether the process of photodetachment was competing, and the thresholds for photodetachment were unknown. By establishing the electron affinities for these iron carbonyls with laser photoelectron

spectrometry, this paper presents the determination of the energy threshold for photodetachment in these anions.

Additionally, the results of this work, combined with earlier mass spectrometric appearance potentials,¹ yield bond strengths of the neutrals. The appearance potentials of Compton and Stockdale provide the bond dissociation strengths of the anions in the process



The bond dissociation energies for the corresponding neutrals may be obtained from a thermodynamic cycle once additional information, the energy needed to remove an electron from each of the anions, is known. This latter information is provided by the electron affinities measured here, and the resulting neutral bond strengths determined by combining the appearance potentials and the electron affinities will be given.

II. Experimental Section

The apparatus and techniques have been previously⁵ described in detail. Iron pentacarbonyl (Apache Chemicals) is dissociated in a low-pressure (1 Torr) electrical discharge ion source to produce beams of Fe^- and $\text{Fe}(\text{CO})_n^-$ ions. The ions are extracted from the source, accelerated to 680 eV, and mass analyzed by a Wien filter. The 0.5–10.0 nA ion beam is crossed in a field-free interaction region by the intracavity beam of a 488-nm (2.540 eV) CW Ar ion laser, and electrons ejected into the acceptance angle of a hemispherical electrostatic monochromator are energy analyzed (resolution 60 meV fwhm). At this resolution the many rotational components of a particular vibronic transition are smoothed into a nearly Gaussian peak 90 meV in width. For the high EA $\text{Fe}(\text{CO})_4$ species, the 363.8-nm lines of an Ar III laser was used.

The absolute, center-of-mass electron kinetic energies of peaks in the detachment spectra are determined using simultaneously produced O^- as a calibration ion and the expression⁵

$$E_X = h\nu - \text{EA}(\text{O}) - 1.0215(\Omega_{\text{O}^-} - \Omega_{\text{X}^-}) - mW(1/M_{\text{O}} - 1/M_{\text{X}}) \quad (1)$$

[†] Department of Chemistry, University of Oregon, Eugene, Oreg. 97403.

* Camille and Henry Dreyfus Teacher-Scholar. Address correspondence to Joint Institute for Laboratory Astrophysics, University of Colorado, Boulder, Colo. 80309.